

See discussions, stats, and author profiles for this publication at: <https://www.researchgate.net/publication/51744469>

# Making a Tool of an Artifact: The Application of Photoinduced Lo Domains in Giant Unilamellar Vesicles to the Study of Lo/Ld Phase Spinodal Decomposition and Its Modulation by the...

ARTICLE *in* LANGMUIR · DECEMBER 2011

Impact Factor: 4.46 · DOI: 10.1021/la203101y · Source: PubMed

---

CITATIONS

7

---

READS

54

5 AUTHORS, INCLUDING:



**Galya Staneva**

Bulgarian Academy of Sciences

43 PUBLICATIONS 342 CITATIONS

SEE PROFILE



**Hélène Conjeaud**

Paris Diderot University

46 PUBLICATIONS 1,736 CITATIONS

SEE PROFILE



**Nicolas Puff**

Pierre and Marie Curie University - Paris 6

27 PUBLICATIONS 295 CITATIONS

SEE PROFILE

# Making a Tool of an Artifact: The Application of Photoinduced Lo Domains in Giant Unilamellar Vesicles to the Study of Lo/Ld Phase Spinodal Decomposition and Its Modulation by the Ganglioside GM1

Galya Staneva,<sup>†</sup> Michel Seigneuret,<sup>\*,‡</sup> H            ,<sup>‡</sup> Nicolas Puff,<sup>‡,  </sup> and Miglena I. Angelova<sup>‡,  </sup>

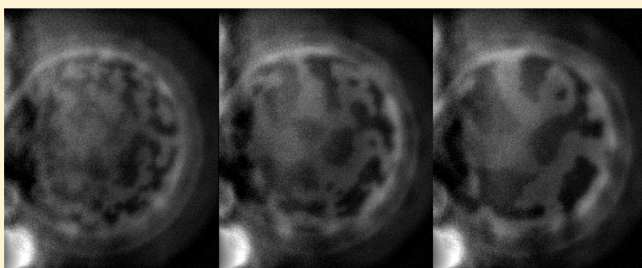
<sup>†</sup>Institute of Biophysics and Biomedical Engineering, Bulgarian Academy of Sciences, Sofia, Bulgaria

<sup>‡</sup>Mati     et Syst            , UMR 7057, Universit     Paris-Diderot & CNRS, Paris, France

<sup>  </sup>UPMC Universit     Paris 6, UFR 925 Physics Department, Paris, France

**S** Supporting Information

**ABSTRACT:** Electroformed giant unilamellar vesicles containing liquid-ordered Lo domains are important tools for the modeling of the physicochemical properties and biological functions of lipid rafts. Lo domains are usually imaged using fluorescence microscopy of differentially phase-partitioning membrane-embedded probes. Recently, it has been shown that these probes also have a photosensitizing effect that leads to lipid chemical modification during the fluorescence microscopy experiments. Moreover, the lipid reaction products are able as such to promote Lo microdomain formation, leading to potential artifacts. We show here that this photoinduced effect can also purposely be used as a new approach to study Lo microdomain formation in giant unilamellar vesicles. Photosensitized lipid modification can promote Lo microdomain appearance and growth uniformly and on a faster time scale, thereby yielding new information on such processes. For instance, in egg phosphatidylcholine/egg sphingomyelin/cholesterol 50:30:20 (mol/mol) giant unilamellar vesicles, photoinduced Lo microdomain formation appears to occur by the rarely observed spinodal decomposition process rather than by the common nucleation process usually observed for Lo domain formation in bilayers. Moreover, temperature and the presence of the ganglioside GM1 have a profound effect on the morphological outcome of the photoinduced phase separation, eventually leading to features such as bicontinuous phases, phase percolation inversions, and patterns evoking double phase separations. GM1 also has the effect of destabilizing Lo microdomains. These properties may have consequences for Lo nanodomains stability and therefore for raft dynamics in biomembranes. Our data show that photoinduced Lo microdomains can be used to obtain new data on fast raft-mimicking processes in giant unilamellar vesicles.



## INTRODUCTION

The components of biological membranes appear to be nonuniformly distributed laterally.<sup>1</sup> Among the various types of membrane domains, several are based on lipid interactions, with the most documented being the so-called lipid rafts.<sup>2,3</sup> Lipid rafts are domains that are enriched in sphingolipids and cholesterol and that recruit or exclude specific transmembrane or peripheral proteins in a modulable manner. These appear to be involved in many biological functions involving cellular activation, transduction, and signaling. One of their principal roles is related to the regulation of the confinement and the mutual interactions of specific membrane-associated proteins implicated in activation and transduction processes. This is achieved in particular through unique size dynamics involving coalescence/disaggregation of lipid rafts as well as by a controlled recycling.<sup>4</sup>

During the last 10 years, electroformed giant unilamellar vesicles (GUVs) containing Lo (liquid-ordered) domains, enriched in sphingolipids and cholesterol, and coexisting with an

Ld (liquid-disordered) phase, have become important tools for the modeling of properties and biological functions of lipid rafts.<sup>5–9</sup> Although GUV Lo domains can only partially mimic the complex features of biomembrane rafts (e.g., heterogeneity of composition, asymmetry, dynamic size distribution, recycling), these have been instrumental in evaluating current ideas as well as in making new proposals for raft-associated mechanisms; for example.<sup>10–12</sup> Lo microdomains (i.e., micrometer-scale domains) are usually imaged in GUVs using fluorescence microscopy of membrane-embedded probes that partition differently and/or fluoresce differently in distinct phases.<sup>5,13,14</sup> One of the topics which has been numerously addressed with such an approach is the dynamics of Lo microdomains formation. The importance of this feature arises from the fact that, in biological

**Received:** August 9, 2011

**Revised:** October 11, 2011

**Published:** October 25, 2011

membranes of “resting” (i.e., nonactivated) cells, rafts are usually not optically detectable. This has suggested that these would exist as nanorafts (i.e., nanometer-scale rafts) that could undergo coalescence into micrometer-sized domains during specific cellular activation processes. This feature may be pivotal to the raft function.<sup>4</sup> The factors affecting Lo domain size and the search for Lo nanodomains (i.e., nanometer-scale domains) as precursors in Lo microdomain formation in model membranes are therefore subjects of intense investigation.<sup>15–20</sup> The usual approach for studying the formation of Lo microdomains in GUVs is to use a range of lipid compositions for their preparation and/or to vary the temperature. These studies have yielded important results, culminating in the determination of several Lo/Ld phase diagrams for specific lipid mixtures.<sup>7,9,18</sup> However, the very dynamics of raft formation and their size modulation in biomembranes, which are taking place in millisecond to second time scales, are still difficult to reproduce in artificial membranes.

In the present work, we propose a simple method which allows one to monitor the dynamics of Lo domain formation in GUVs on a faster time scale. This approach involves inducing a fast in situ modification of the membrane lipid chemical composition. The method originates from the photosensitizing effect of the fluorescent probes used for Lo domain detection in GUVs, occurring during the fluorescence microscopy experiments. According to two recent reports by Ayuyan and Cohen<sup>21</sup> and by Feigenson and collaborators,<sup>22</sup> such a photosensitization leads to production of free radicals, including reactive oxygen species, and to lipid chemical modification(s). The resulting lipid reaction products are able as such to promote Lo microdomain formation. While Ayuyan and Cohen<sup>21</sup> have shown that sphingomyelin peroxides are formed and point to their role in this process, Feigenson et al.<sup>22</sup> also propose that lipid oligomers, promoted by free radical-induced double bond dimerization, might play a role. In any case, it has been emphasized that this effect may lead to artifacts in studies of Lo domains in GUVs. Approaches to overcome these pitfalls have been suggested.<sup>21,23</sup> Although photosensitization-induced Lo domain formation must indeed be avoided in most cases, we show here that it can also be purposely used since it provides a way to trigger raft-type microdomain appearance in GUVs on a faster time scale, relevant to cellular activation phenomena, and to study the effect of any parameter on such a process. We illustrate the usefulness of this approach by studying the dynamics and phase morphologies of Lo microdomain formation in GUVs and the influence of the ganglioside GM1 thereupon. Gangliosides are essential components of rafts and are directly involved in several raft-associated cellular processes.<sup>24,25</sup> Although GM1 has been used in GUVs for Lo domains labeling purposes<sup>5,26</sup> or to study cholera toxin-induced Lo domain coalescence,<sup>27</sup> its role on Lo domains formation, stability, and dynamics has up to now not been studied.

## MATERIALS AND METHODS

**Reagents.** Lipids were obtained as follows and used without further purification: egg yolk 1- $\alpha$ -phosphatidylcholine (PC), egg yolk sphingomyelin (SM), cholesterol (Chol), and ovine brain GM1 were from Avanti; the fluorescent lipid analogue Texas Red DPPE (TR-PE) was from Invitrogen.

**Vesicle Preparation.** GUVs were made by the electroformation method on platinum electrodes in a temperature-controlled chamber following a particular protocol previously described using an AC peak to peak tension lower than 1 V.<sup>10,11,28</sup>

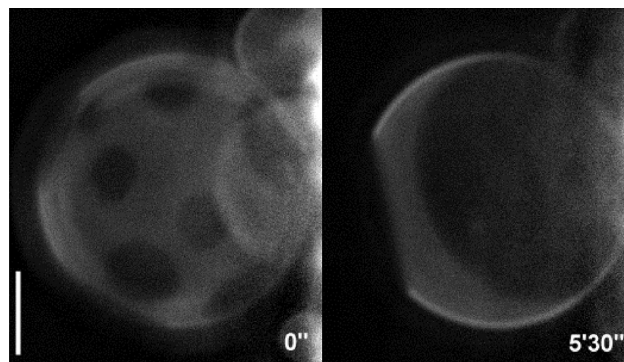


**Figure 1.** Time-dependent evolution at 19 °C of pre-existing light-insensitive Lo domains present on GUVs with molar composition PC/SM/CHOL 50:30:20 and labeled with TR-PE (0.25% mol percentage). The elapsed time after the beginning of movie acquisition is indicated for both images. Scale bar = 10  $\mu$ m.

**Video Microscopy.** A Zeiss Axiovert 200 M microscope (fluorescent unit fluo arc N HBO 103, Zeiss), equipped with a Lambda 10-2 unit (Sutter Instrument Co.), plus a CCD B/W chilled camera (Cool SNAP HQ), was used for GUV imaging. The setup was computer-controlled by the Metamorph 6.0 software (Roper Sci.). A 40 $\times$  Ph LD Zeiss objective was used. The morphology transformations and dynamics of the heterogeneous GUV membranes were followed by fluorescence using Zeiss filter set 15 (Ex/Em = 550/620 nm). Most studies were performed using the minimum intensity of the HBO lamp (25 W), while a few studies used higher intensities up to 100 W. Fluorescence imaging microscopy experiments used image acquisition times under illumination ranging from 0.3 to 0.6 s and repetition times in the dark of 2 s. In all shown image series and movies, film acquisition was started immediately from the beginning of illumination.

**Image Processing and Quantitative Analysis.** Image processing was done with ImageJ.<sup>29</sup> Image and movies were background-corrected with the “subtract background” routine. Individual images were further processed with the “unsharp mask” filter. To quantify Lo/Ld phase separation and its kinetics, the broadening of the pixel intensity distribution of successive images in films was computed. For the purpose of extracting the pixel intensity distribution from the image series, the following procedure was used. All images were first negativized. A mask was constructed and all images were cropped to eliminate the fluorescence arising from the electrode and the vesicle periphery and then denegativized. All images were normalized to a reference image chosen before the onset of phase separation (it was checked that the results are independent of the exact chosen image). The average pixel intensity value, the standard deviation of pixel intensities, and the standard deviation normalized to the average were calculated for each of a number of images at fixed interval in the thereby processed phase separation film. The method is illustrated in Figure S1 (Supporting Information). This analysis also indicated that the average pixel intensity value of each GUV remains constant throughout the experiment (Figure S1C, Supporting Information), suggesting that probe photobleaching was not significant.

## RESULTS AND DISCUSSION

GUVs were prepared with the starting molar composition PC/SM/CHOL 50:30:20. This composition was chosen because it yields Lo microdomains below 23 °C.<sup>30</sup> In experiments described below, GM1 was substituted for SM in proportions from 1 to 10. Texas red phosphatidylethanolamine (TR-PE) was used as a probe. It partitions in favor of the Ld phase<sup>5</sup> which

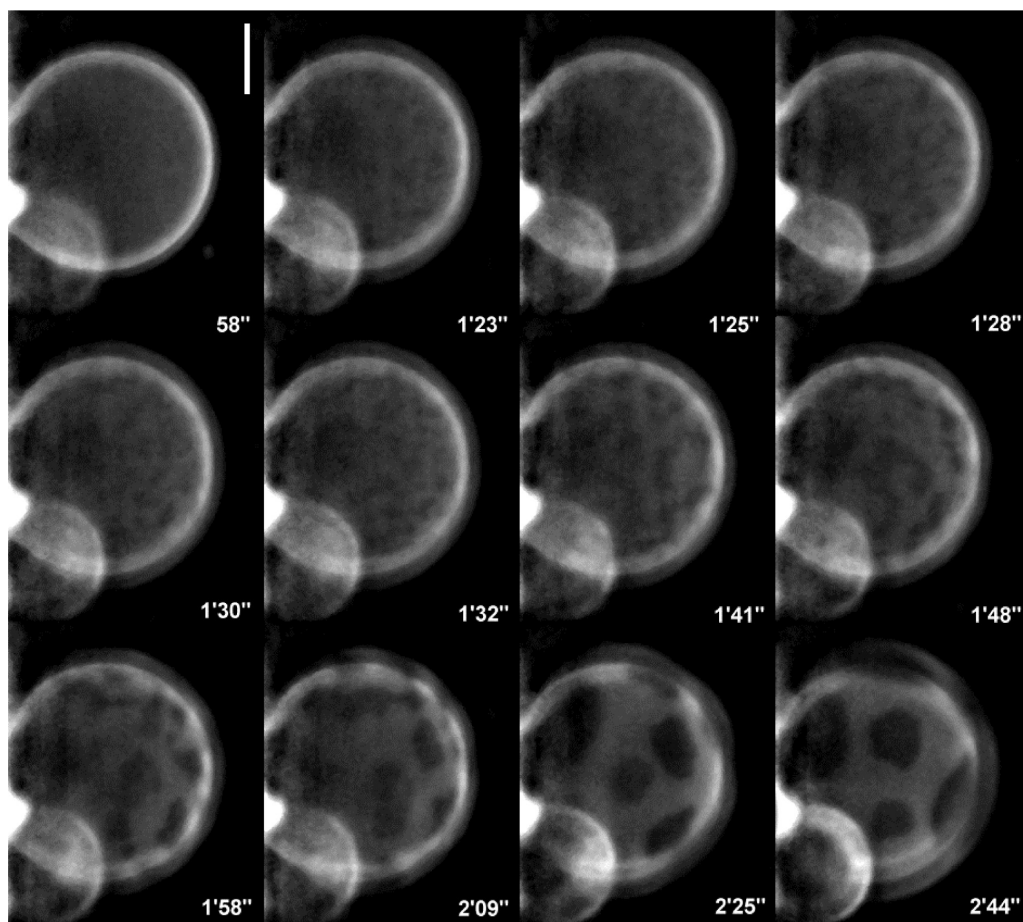


**Figure 2.** Time-dependent development of photoinduced phase separation and Lo domain formation at 24 °C on a single GUV with molar composition PC/SM/CHOL 50:30:20 and labeled with TR-PE (0.25% mol percentage) illustrating the spinodal decomposition process. The elapsed time after the beginning of movie acquisition is indicated for each image. Scale bar = 10  $\mu\text{m}$ .

appears brighter while the Lo phase appears darker by fluorescence microscopy. The probe concentration was usually 0.25% (mol/mol), although higher concentrations were occasionally used with a parallel decrease of the PC molar fraction. This low probe concentration, combined with the limited excitation light intensities (see Materials and Methods), which both will be accounted for below, explain the limited signal-to-noise ratio of the data presented here. As expected,<sup>30</sup> below 23 °C, fluorescence microscopy of these GUVs shows the occurrence of pre-existing micrometer-sized Lo domains that ultimately transform into a single cap at such temperatures in times ranging from 3 to 6 min (Figure 1).

Oppositely, GUVs initially displaying an homogeneous Ld phase are observed at higher temperatures. However, above 23 °C, when an initially homogeneous Ld phase vesicle is continuously imaged under repetitive transient fluorescence excitation light, Lo domains appear, after a lag period, on the whole visible surface of the vesicle and grow in size over the continuous Ld phase. Figure 2 and Movie S1 (Supporting Information) illustrate this process. Figure 3 shows the kinetics of appearance of the dark domains (as measured through the distribution width of pixel intensities of successive images; see Materials and Methods and Figure S1, Supporting Information). In agreement with previous studies,<sup>21,22</sup> we attribute this Lo domain growth as originating from photosensitization. During the transient illumination phases of time lapse imaging,

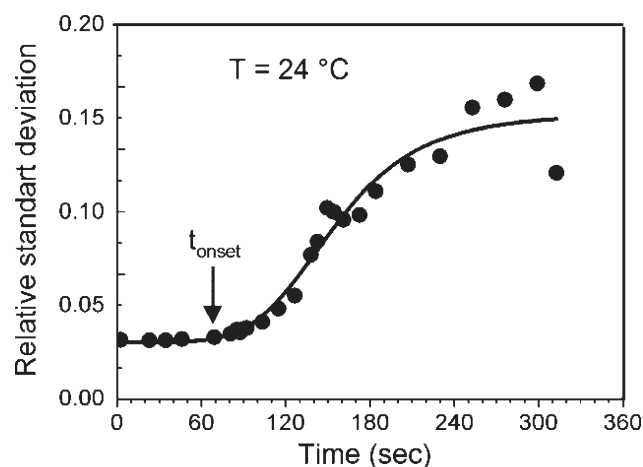


**Figure 3.** Kinetics of phase separation on the GUV sample of Figure 2, as measured by evolution of the relative mean square deviation of fluorescence image pixel intensity vs time (Figure S1, Supporting Information). Time zero corresponds to the beginning of movie acquisition and transient illumination.

the excited fluorescence probe generates free radicals which covalently alter lipids, yielding molecular species that favor Lo domain formation.



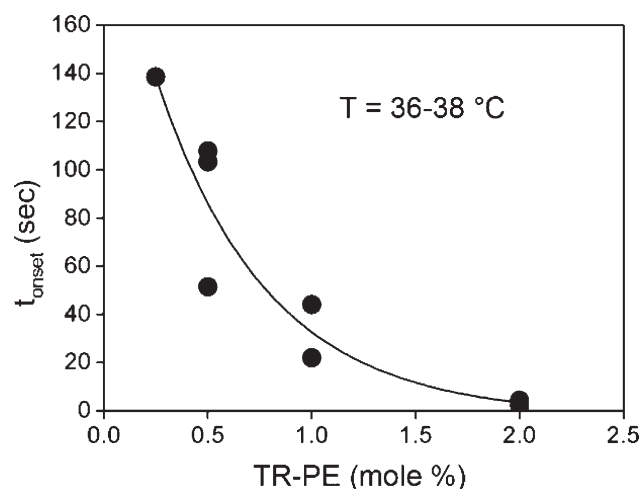


**Figure 4.** Dependence of the onset time for photoinduced phase separation GUVs with molar composition PC/SM/CHOL 50:30:20 at 36–38 °C upon TR-PE mole percent at constant excitation light intensity. Each point corresponds to a different GUV sample. Increase in probe concentration was compensated by a corresponding decrease of the PC concentration. The excitation light intensity was kept constant at 25 W of the HBO lamp. Similar image acquisition times under illumination were used in all experiments. The onset time (or lag time)  $t_{\text{onset}}$  was calculated as indicated in Figure S1, Supporting Information.

In our case, this is borne out by the fact that the onset time ( $t_{\text{onset}}$  or lag period) for appearance of dark domains decreases with increasing fluorescence probe concentration at constant excitation light intensity (Figure 4). The onset time for phase separation also decreased with increasing excitation light intensity (at identical image acquisition times), down to less than 1 s or below at the maximum intensity of our setup (not shown). This indicates that Lo microdomain formation can be triggered within a 1 s time scale with standard equipment under adequate experimental conditions. Here, in order to follow the kinetics of photoinduced Lo domain formation with sufficient accuracy, a probe concentration of 0.25% and a low light intensity were chosen in further experiments.

The onset and evolution of the photoinduced Lo/Ld phase separation occurring above 23 °C is morphologically different from the usual growth pattern observed for Lo domain formation induced by, for example, lowering the temperature. In the usual case, Lo microdomains grow by a typical nucleation process in which a limited number of discrete round spots appear at discrete loci, increase in size, and fuse into larger domains<sup>31</sup> (a pattern evolution which is observed here below 23 °C; see Figure 1). Oppositely, for the photoinduced Lo/Ld phase separation observed above 23 °C, small irregularly shaped dark domains appear uniformly on the whole visible surface of the vesicle, grow, and progressively transform into elongated strips and then into oval and nearly round domains (Figure 2). This suggests that photoinduced Lo domain formation occurs by spinodal decomposition. Spinodal decomposition takes place when an initially miscible multicomponent system is rapidly brought within a specific range of temperature/composition (delimited by the so-called spinodal curve of the phase diagram), which corresponds to unstable demixing conditions (as opposed to nucleation for which demixing conditions are metastable).<sup>32,33</sup> Unlike nucleation, phase separation by spinodal decomposition occurs uniformly in the system. It is due to the growth of compositional

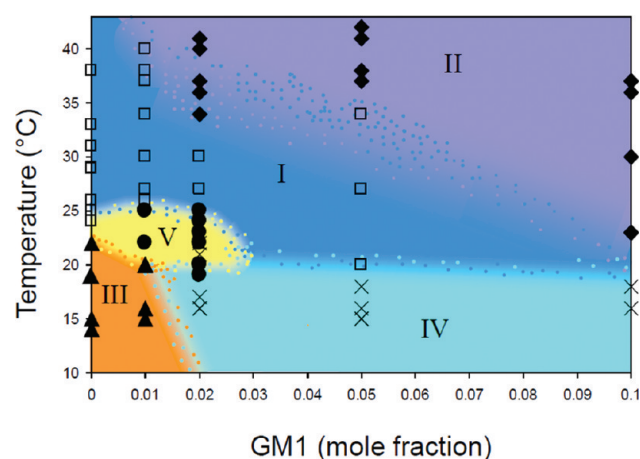


**Figure 5.** Phase behavior of PC/SM/CHOL/GM1 GUVs as a function of temperature and GM1 mol fraction presented as a morphology diagram. Each point corresponds to the evolution of a single GUV, and data are gathered from two or three different samples for each GM1 concentration. All data was recorded at 0.25% mol percent TR-PE and 25 W light intensity of the HBO lamp. Each region represents one type of Lo/Ld phase morphology evolution under illumination. Region I (blue, open squares), photoinduced spinodal decomposition leading to formation of discrete Lo microdomains over an Ld phase; region II (mauve, filled tilted squares), absence of phase separation, that is, homogeneous Ld phase vesicles; region III (orange, filled triangles), preformed Lo microdomains over an Ld phase; region IV (cyan, crosses), photoinduced spinodal decomposition leading to percolation inversion and formation of discrete Ld microdomains over a an Lo phase; region V (yellow, filled circles), photoinduced spinodal decomposition leading to simultaneous large Lo phase areas containing small Ld domains and large Ld phase areas containing small Lo domains.

heterogeneity within a specific size range of fluctuations, thereby forming domains which increase in size. The initial size range and demixing amplitude as well as their growth rate are determined by the antagonism between the negative (favorable) phase separation free energy and the positive (unfavorable) boundary energy (e.g., surface or line tension). Spinodal decomposition is usually promoted “vertically”, that is, by relatively rapid temperature quenching below the spinodal curve. Veatch and Keller observed one such condition for Lo/Ld phase separation in DOPC/DPPC/Chol GUVs near a critical point.<sup>34</sup> In our case, the process occurs “horizontally”, that is, by change of chemical composition at constant temperature, with relatively fast formation of photoinduced lipid byproducts promoting Lo domain formation by reaching the spinodal region. A difference between the two processes is that the photoinduced spinodal decomposition proceeds after an onset time (except at high fluorescence probe concentration or light excitation intensity). This likely represents the necessary time (i.e., the necessary number of illumination transients) to reach a threshold concentration of the modified lipid species responsible for Lo domain formation. The fact that spinodal decomposition actually occurs in our experiments is confirmed by the irregular boundaries of the initial dark domains (Figure 2). Indeed, the boundary shape corresponds to an interplay between entropic factors, that favor fluctuating irregular contours, and positive boundary energy (i.e., line tension) that tend to minimize such contours. During the first stages of spinodal decomposition, the two separating phases have very similar chemical composition so that line tension is weak leading to unstable domain contours. As expected, spinodal

decomposition proceeds into coarsening, that is, size increase and decrease in number of the domains.<sup>33</sup> Domains, while becoming larger, also become sharper and rounder in boundaries, due to the increase of line tension since larger compositional heterogeneity occurs as phase separation increases. In other instances of spinodal decomposition, coarsening eventually leads to the transient or permanent formation of a bicontinuous phase (i.e., a semi-interpenetrating network of two phases<sup>35</sup>) if the proportions of the two phases are comparable, a situation

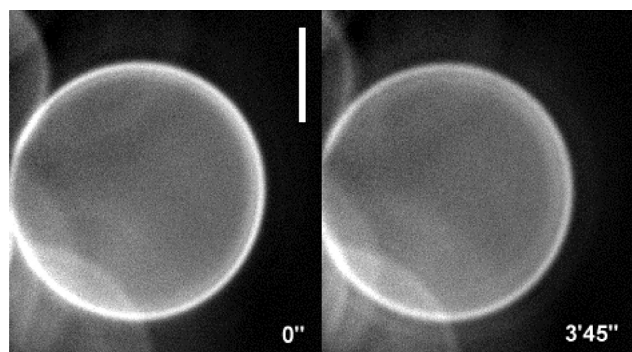


**Figure 6.** Absence of photoinduced phase separation at 37 °C on an homogeneous Ld phase GUV with molar composition PC/SM/CHOL/GM1 50:28:20:2 and labeled with TR-PE (0.25% mol percent). The elapsed time after the beginning of movie acquisition is indicated for both images. Scale bar = 10  $\mu$ m.

which has been termed “critical composition”.<sup>33,35–37</sup> Spinodal decomposition has also recently been described in the framework of percolation theory in which the bicontinuous phase corresponds to the “percolation threshold” for percolation inversion (i.e., inversion of the infinite phase and the phase in domains).<sup>38</sup> This does not occur here in the absence of GM1, and the final morphology corresponds to discrete Lo domains over a continuous Ld phase eventually forming a cap (see movie S1, Supporting Information). This is presumably due to the fact that the surface fraction of the Lo phase is too low in this temperature range so that the mixture is “off-critical”<sup>33,35–37</sup> and that a percolation threshold<sup>38</sup> is not reached (however see below).

Interestingly, below 23 °C, when Lo domains preformed in the dark (by nucleation) are present before the beginning of illumination, the appearance of photoinduced Lo domains is never observed (Figure 1, note that care was taken to use a nonilluminated region for each observation and to start the recording immediately after the start of illumination). This is likely due to the fact that lipids essential to Lo domain formation, that is, sphingomyelin and cholesterol, are already extensively sequestered in the pre-existing Lo domains and therefore unavailable for photoinduced Lo domain formation.

The presence of GM1 was found to have a profound influence on the light induced Lo phase formation and its temperature dependence. In Figure 5, we have tentatively summarized the different types of evolutions of phase separation morphologies, as a function of the GM1 molar ratios and temperature in the form of a morphological diagram with approximate continuous

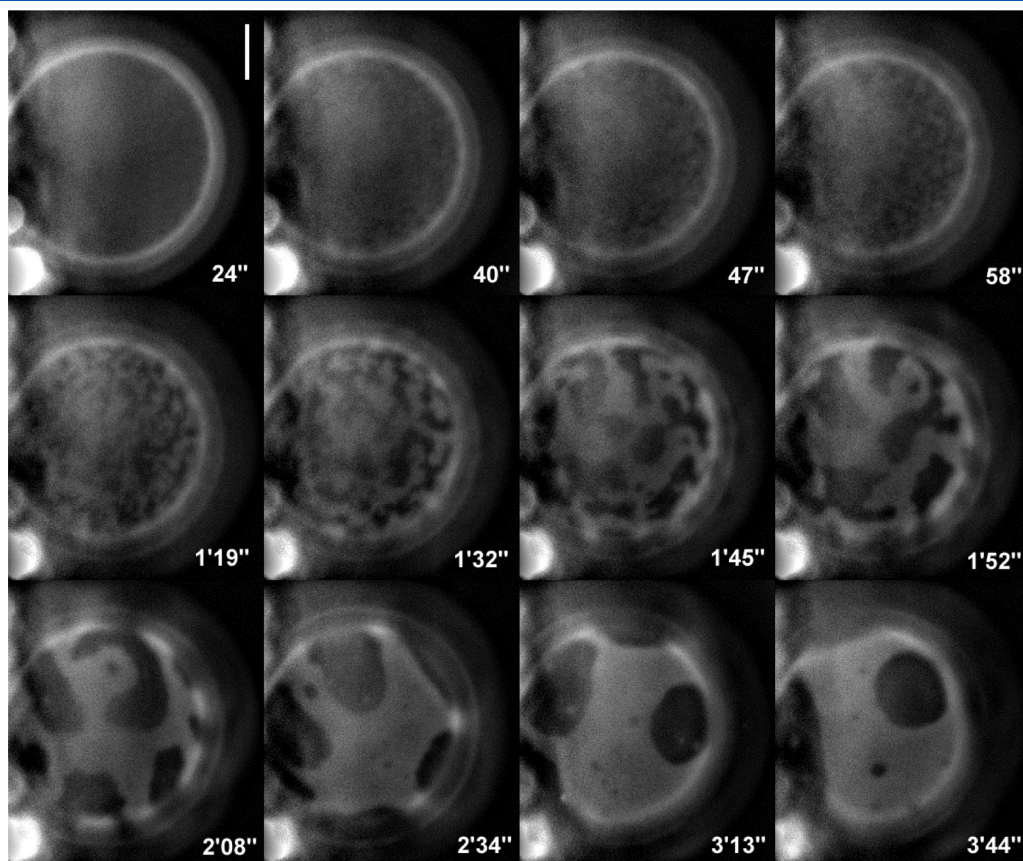


**Figure 7.** Time-dependent development of photoinduced Lo/Ld phase separation at 27 °C on a single GUV with composition PC/SM/CHOL/GM1 50:28:20:2 and labeled with TR-PE (0.25% mol percent) illustrating a spinodal decomposition process similar to that observed in the absence of GM1 (region I in Figure 5). The elapsed time after the beginning of movie acquisition is indicated for each image. Scale bar = 10  $\mu$ m.



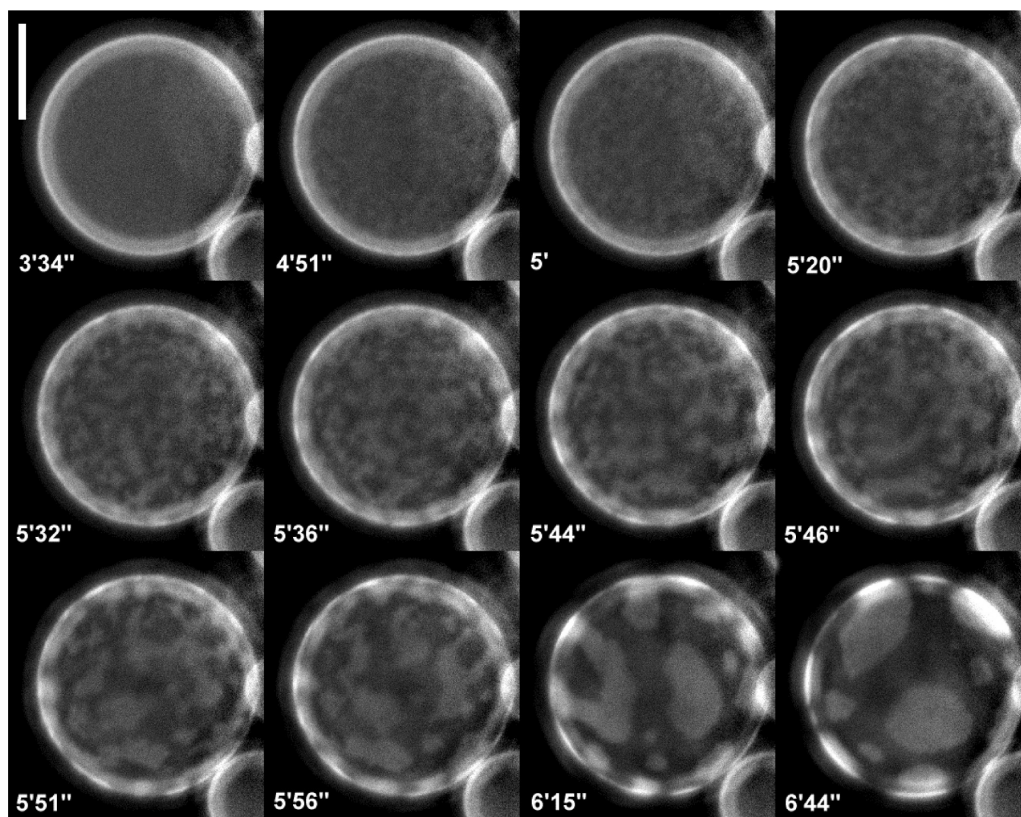


**Figure 8.** Time-dependent development of photoinduced Lo/Ld phase separation at 20 °C on a GUV with molar composition PC/SM/CHOL/GM1 50:28:20:2 labeled with TR-PE (0.25% mol percent) illustrating a percolation inversion process (region IV in Figure 5). The elapsed time after the beginning of movie acquisition is indicated for each image. Scale bar = 10  $\mu$ m.

boundaries. Indeed, although the observed effects on phase separation morphology were qualitatively reproducible, the temperature limit for each morphology was found to vary by a few degrees from sample to sample with identical starting composition. This is presumably due to slight differences in final lipid compositions inherent to preparation of GUVs from a dry lipid film.<sup>7</sup> Each type of morphology evolution is illustrated in the following image series and films. A first obvious effect is that GM1 hinders the formation of photoinduced Lo microdomains. Indeed the maximum temperature at which photoinduced Lo microdomains are observed was found to decrease with increasing GM1 content above 1%. While a photoinduced phase separation similar to that observed at 0% GM1 is still observed (region I of Figure 5), its maximum temperature of occurrence is decreased with increasing GM1. Above such a temperature, homogeneous Ld vesicles are observed that do not display photoinduced phase separation even after several minutes of illumination. This corresponds to region II in Figure 5 and is illustrated in Figure 6. Noteworthy, GM1 also hinders the formation of the preformed light-independent Lo domains observed at lower temperature between 15 and 23 °C (region III of Figure 5). These are no more observed above 1% GM1. A consequence of this latter effect is that the temperature range of photoinduced Lo domain formation is extended to lower temperature. This confirms the idea that the nonappearance of photoinduced Lo microdomains at low temperature in the absence of GM1 is due to sequestering of mandatory lipids in preformed Lo domains.

A consequence of this extension of the range of photoinduced phase separation to lower temperature is that a more diverse manifold of phase morphology evolutions can be observed.

Although photoinduced Lo/Ld phase separation is still invariably initiated by spinodal decomposition (suggesting that GM1 does not influence qualitatively the photosensitization and lipid modification processes), its morphological outcome depends both on GM1 content and temperature. Above 20–25 °C, in the presence of GM1, the photoinduced phase separation process occurs similarly to what is found without GM1, namely, small irregular dark domains that appear on the whole visible surface of the vesicle, grow, and progressively evolve into oval and nearly round dark Lo domains on a bright Ld phase background, never attaining a bicontinuous phase stage. This corresponds to region I of Figure 5 and is illustrated in Figure 7 and Movie S2 (Supporting Information). The kinetics of photoinduced spinodal decomposition is comparable to that found in the absence of GM1 ( $t_{\text{onset}} = 38$  s at 27 °C in Figure 7 and 68 s in Figure 2 at 24 °C), again suggesting that GM1 does not influence importantly the photosensitization and lipid modification processes. On the other hand, below such temperatures, the morphology evolution is partially different. This corresponds to region IV in Figure 5 and is illustrated in Figure 8 and Movie S3 (Supporting Information). Here, while spinodal decomposition takes place and small irregular dark Lo domains initially appear similarly and undergo coarsening, here this coarsening does proceed to formation of a bicontinuous phase, due to rapid coalescence of the Lo domains. This coalescence ultimately leads to a percolation of the Lo phase and a depercolation of the Ld phase so that bright round Ld domains over a dark Lo phase are ultimately observed. An obvious explanation for this percolation inversion behavior is that, below a specific temperature,

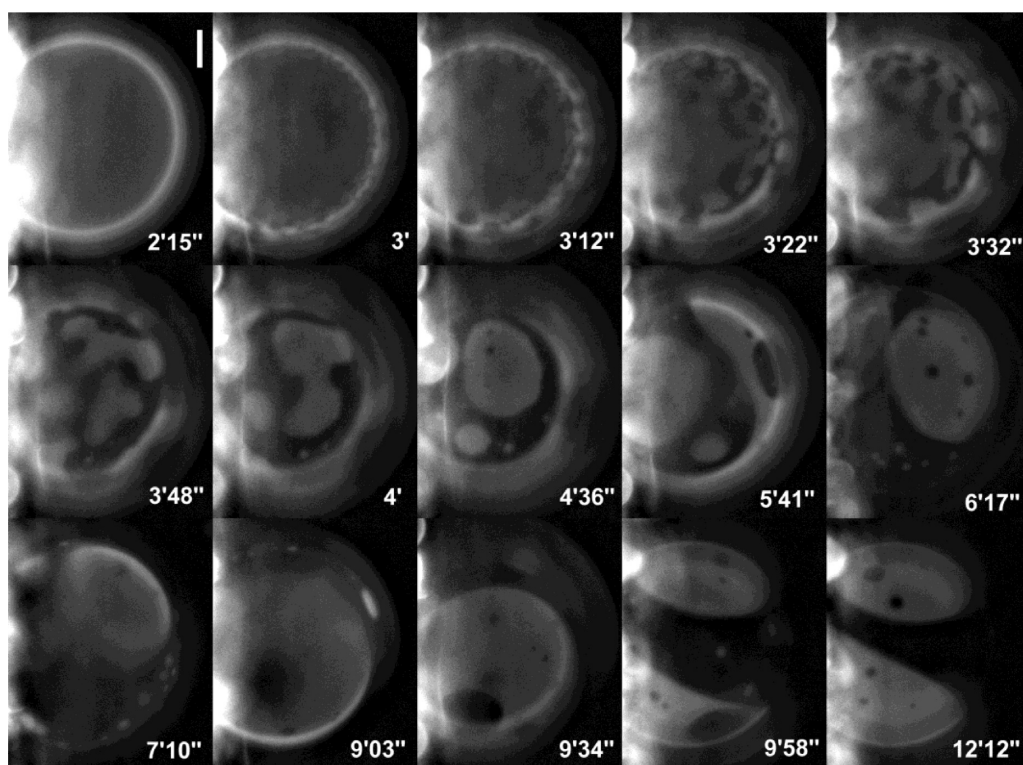


**Figure 9.** Time-dependent development of photoinduced Lo/Ld phase separation at 23 °C on a GUV with composition PC/SM/CHOL/GM1 50:28:20:2 and labeled with TR-PE (0.25% mol percent) illustrating the formation of a morphology involving simultaneous large Lo phase areas containing small Ld domain and large Ld phase areas containing small Lo domains (region V in Figure 2). The elapsed time after the beginning of movie acquisition is indicated for each image. Scale bar = 10  $\mu$ m.

the Lo phase ultimately becomes the major contributing phase. Therefore, a reversed off-critical composition is reached<sup>33,35–37</sup> and a percolation threshold<sup>38</sup> is attained and overpassed.

The transition between these two patterns of phase morphology evolution (i.e., evolution toward discontinuous Lo domains over continuous Ld phase and vice versa) occurs abruptly at a defined temperature boundary at ca. 20 °C for all GM1 concentrations above 2% (Figure 5). Interestingly, this boundary temperature is independent of the GM1 content above 2%, suggesting that GM1 does not hinder the conversion from photoinduced Lo microdomain to bulk Lo phase as it does for the formation of these photoinduced Lo microdomains. Strikingly, around 1–2% GM1, a limited region occurs in which another different long-term phase separation behavior is apparent. This corresponds to region V in Figure 5. Such a behavior is illustrated in Figure 9 and Movie S4 (Supporting Information). Another example is shown in Figure S2 and Movie S5 (Supporting Information). In this specific region, spinodal decomposition does occur, proceeding to coarsening into a bicontinuous phase. However, here the system does not reach percolation inversion. There is a progressive evolution toward a particular morphology with intertwined stripes of each phase growing in size presumably due to line tension effects, and containing small domains of the other phase. This leads to a final situation where there is a coexistence and a constant dynamical remodeling of large capped or annular domains of both Ld and Lo phase encompassing the vesicle surface. There are therefore simultaneously large Lo phase areas containing small Ld domains and large Ld phase areas containing small Lo domains in a constantly remodeling pattern. A final steady cap

morphology is never observed. It is likely that such a behavior corresponds to a “critical” compositional region of the two phases<sup>33,35–37</sup> situated in the vicinity of the percolation threshold.<sup>38</sup> Noteworthy, the morphology evolution observed here is reminiscent of the vertical spinodal decomposition process evidenced by Veatch and Keller<sup>34</sup> and simulated by Camley and Brown.<sup>39</sup> The final morphology of the phase separation in this specific region also evokes patterns termed “double phase separation processes” already observed or simulated for specific 2D fluid mixtures.<sup>40,41</sup> This final dynamical morphology likely corresponds to a complex interplay between line tension, viscoelastic properties, and confinement effects occurring within this specific range of GM1 concentrations.

## CONCLUSION

Although photoinduced Lo domain formation has already been studied in much detail as a potential artifact in two previous publications,<sup>21,22</sup> the present work considers this process from a very different perspective. Our study indicates that photoinduced Lo domain formation in GUVs can be used as a method to mimic fast lipid raft formation processes in artificial membranes. Although raft formation in biomembranes takes place by different mechanisms (e.g., in situ lipid enzymatic modification, carrier vesicle fusion, membrane protein palmitoylation), our method allows one to reproduce in GUVs the fast (second or subsecond time scale) dynamics of such formation. Application of the method in biomembranes might be complicated by photosensitization effects on proteins and membrane recycling processes. On the other hand, since photoinduced Lo domains appear to



form in GUVs with PC/SM/Chol<sup>21</sup> and PC/SM/GM1/Chol (this study) lipid mixtures, as well as with those containing saturated and unsaturated PCs with cholesterol,<sup>22</sup> the method is likely applicable to most types of GUVs containing Lo domain-forming lipids. Very rapid formation of Lo domains can be achieved in GUVs if a few percent of photosensitizing fluorescence probe is used and the method could further benefit from the use of pulse and/or localized illumination methods. This approach involves inducing a fast in situ modification of the membrane lipid chemical composition. Of course, a detailed knowledge of the covalently modified lipid products involved in photoinduced Lo domain formation is necessary. Ayuyan and Cohen<sup>21</sup> have shown that SM-peroxide derivatives are produced, that might react with other lipids. Zhao et al.<sup>22</sup> have additionally suggested a role for polymerized lipids. Such modifications might promote Lo domain formation either by a direct effect of the modified lipid species on lipid order or by changing the proportions of unaltered lipid species.

The possibility to obtain new data by this approach is illustrated here by the observation that, with the specific lipid compositions studied here, such fast photoinduced Lo domain formation appears to occur invariably by spinodal decomposition rather than by the nucleation process previously observed in most Lo/Ld phase separation GUV studies. The fact that photoinduced Lo domain formation occurs by spinodal decomposition may be related to the fact that the change in lipid composition promoted by photosensitization occurs not only rapidly but also uniformly in the GUV bilayer, unlike nucleation which is promoted locally by defects. However, we would like to emphasize that photoinduced Lo domain formation may occur by different mechanisms for other lipid mixtures. Indeed, previous data<sup>21,22</sup> indicate that a more common mechanism is uniform appearance of small round domains that fuse into larger areas (although features evoking spinodal decomposition, i.e. irregular or stripped domains, are occasionally displayed in these two studies). The outcome of photoinduced phase separation likely depends on the status of lipid mixing before illumination, that is, proximity from the (micrometer-scale) demixing region and, in particular, from the critical point (with inherent associated fluctuations<sup>42</sup>), or occurrence of pre-existing nanodomains.<sup>20</sup> Such an outcome also depends also likely upon the modifications of such mixing status during illumination, that is, possible evolution of the newly forming mixture toward the nucleation or the spinodal demixing regions.

Although, spinodal decomposition processes in lipid bilayers have been numerous studied theoretically or simulated,<sup>39,43–48</sup> previous experimental examples are scarce.<sup>34</sup> The photoinduced Lo domain formation method potentially provides a simple controllable approach to evaluate these theories. In this instance, to our knowledge, our study is the first to document experimentally the various morphological outcomes of spinodal decomposition in bilayers under critical and off-critical conditions. Interestingly, photoinduced phase separation of Lo domains has also recently been used as a tool to promote lipid sorting and morphology changes in tubules.<sup>49</sup>

Since raft formation may occur rapidly in biomembranes, the biological implications of such spinodal processes should be considered. The spinodal decomposition mechanisms observed here may be relevant to the process of putative nanodomain formation in heterogeneous GUVs or in biomembranes. Interestingly, spinodal decomposition intrinsically contains the notion of nanodomains since it is initiated by growth of a specific size range of nanoscale compositional fluctuations that consolidate into

domains.<sup>32,33</sup> Studies on other system types indicate that spinodal decomposition can be “arrested” at specific growth stages by various factors.<sup>50–52</sup> Stabilization of nanodomains in GUVs and biomembrane may be related to arrested spinodal decomposition. For instance, theoretical work by Frolov et al.<sup>53</sup> suggests that nanodomain stabilization may occur in bilayers as a consequence of both entropic effects and low line tension.

In this instance, it is interesting to discuss the effect of GM1. GM1 appears to specifically hinder the formation of Lo microdomains. Indeed a decrease of the maximum temperature at which both “darkness” preformed Lo microdomains and photoinduced Lo microdomains become apparent is observed with increasing GM1 concentrations. Previous studies suggest that GM1 partitions almost exclusively in Lo domains.<sup>26,54</sup> Therefore, two explanations are possible for the effect of GM1 on Lo microdomain formation. One is that GM1 intrinsically destabilizes the Lo phase due to weaker interaction with other lipids, for example, that GM1–cholesterol interactions are weaker than SM–cholesterol interactions. While this explanation cannot be excluded, this does not seem in agreement with current comparative thermotropic data on these interactions.<sup>55</sup> Additionally, our study suggests that GM1 hinders formation of isolated Lo microdomains and not formation of a bulk Lo phase from microdomains. Therefore, another explanation is that GM1 could “arrest” Lo domain growth through a decreasing effect on the line tension between the Lo and Ld phase. This would therefore stabilize Lo nanodomains and thereby hinder the formation of Lo microdomains. A speculative explanation for such an effect would be that GM1 molecules located at domain boundaries would stabilize highly curved nanodomain interfaces due to mutual electrostatic repulsion associated with the charged and bulky headgroup. GM1 would therefore act as a linactant, that is, a 2D surfactant.<sup>56,57</sup> Studies by nanoscale methods (e.g., AFM, FRET) of the earliest stage of photoinduced spinodal decompositions before the appearance of microdomains may help evaluate this hypothesis.

## ■ ASSOCIATED CONTENT

**S Supporting Information.** Figure documenting the method used for kinetic analysis of Lo/Ld phase separation. Additional image series of photoinduced Lo/Ld phase separation. Movies corresponding to the different morphological evolutions of photoinduced Lo/Ld phase separation. This material is available free of charge via the Internet at <http://pubs.acs.org>.

## ■ AUTHOR INFORMATION

### Corresponding Author

\*E-mail: [michel.seigneuret@univ-paris-diderot.fr](mailto:michel.seigneuret@univ-paris-diderot.fr).

## ■ ACKNOWLEDGMENT

We are indebted to Dr. Jean-Baptiste Fournier and Dr. Masayuki Imai for helpful discussions. This work was supported by grants from the CNRS (UMR 7057), the Université Paris-Diderot, and the Bulgarian Fund for Scientific Research (DTK02/5-2009).

## ■ REFERENCES

- (1) Lindner, R.; Naim, H. Y. *Exp. Cell. Res.* **2009**, *315*, 2871.
- (2) Simons, K.; Ikonen, E. *Nature* **1997**, *387*, 569.
- (3) Brown, D. A.; London, E. J. *Biol. Chem.* **2000**, *275*, 17221.

- (4) Simons, K.; Gerl, M. J. *Nat. Rev. Mol. Cell. Biol.* **2010**, *11*, 688.
- (5) Dietrich, C.; Bagatolli, L. A.; Volovyk, Z. N.; Thompson, N. L.; Levi, M.; Jacobson, K.; Gratton, E. *Biophys. J.* **2001**, *80*, 1417.
- (6) London, E. *Biochim. Biophys. Acta* **2005**, *1746*, 203.
- (7) Veatch, S. L.; Keller, S. L. *Biochim. Biophys. Acta* **2005**, *1746*, 172.
- (8) Angelova, M. I.; Puff, N.; Seigneuret, M. In *Biochemistry and Biophysics of Lipids*; Pramanik, A., Ed.; Research Signpost: Trivandrum, 2006; p 1.
- (9) Feigenson, G. W. *Biochim. Biophys. Acta* **2009**, *1788*, 47.
- (10) Staneva, G.; Angelova, M. I.; Koumanov, K. *Chem. Phys. Lipids* **2004**, *129*, 53.
- (11) Staneva, G.; Seigneuret, M.; Koumanov, K.; Trugnan, G.; Angelova, M. I. *Chem. Phys. Lipids* **2005**, *136*, 55.
- (12) Kahya, N. *Chem Phys Lipids* **2006**, *141*, 158.
- (13) Heberle, F. A.; Buboltz, J. T.; Stringer, D.; Feigenson, G. W. *Biochim. Biophys. Acta* **2005**, *1746*, 186.
- (14) Baumgart, T.; Hunt, G.; Farkas, E. R.; Webb, W. W.; Feigenson, G. W. *Biochim. Biophys. Acta* **2007**, *1768*, 2182.
- (15) Veatch, S. L.; Polozov, I. V.; Gawrisch, K.; Keller, S. L. *Biophys. J.* **2004**, *86*, 2910.
- (16) Feigenson, G. W.; Buboltz, J. T. *Biophys. J.* **2001**, *80*, 2775.
- (17) Silvius, J. R. *Biophys. J.* **2003**, *85*, 1034.
- (18) Feigenson, G. W. *Annu. Rev. Biophys. Biomol. Struct.* **2007**, *36*, 63.
- (19) Bunge, A.; Müller, P.; Stöckl, M.; Herrmann, A.; Huster, D. *Biophys. J.* **2008**, *94*, 2680.
- (20) Heberle, F. A.; Wu, J.; Goh, S. L.; Petruziello, R. S.; Feigenson, G. W. *Biophys. J.* **2010**, *99*, 3309.
- (21) Ayuyan, A. G.; Cohen, F. S. *Biophys. J.* **2006**, *91*, 217.
- (22) Zhao, J.; Wu, J.; Shao, H.; Kong, F.; Jain, N.; Hunt, G.; Feigenson, G. W. *Biochim. Biophys. Acta* **2007**, *1768*, 2777.
- (23) Morales-Pennington, N. F.; Wu, J.; Farkas, E. R.; Goh, S. L.; Konyakhina, T. M.; Zheng, J. Y.; Webb, W. W.; Feigenson, G. W. *Biochim. Biophys. Acta* **2010**, *1798*, 1324.
- (24) Sonnino, S.; Prinetti, A. *Adv. Exp. Med. Biol.* **2010**, *688*, 165.
- (25) Gupta, G.; Suroli, A. *FEBS Lett.* **2010**, *584*, 1634.
- (26) Kahya, N.; Scherfeld, D.; Bacia, K.; Poolman, B.; Schwille, P. *J. Biol. Chem.* **2003**, *278*, 28109.
- (27) Hammond, A. T.; Heberle, F. A.; Baumgart, T.; Holowka, D.; Baird, B.; Feigenson, G. W. *Proc. Natl. Acad. Sci. U.S.A.* **2005**, *102*, 6320.
- (28) Angelova, M.; Dimitrov, D. *Faraday Discuss. Chem. Soc.* **1986**, *81*, 303.
- (29) Abramoff, M. D.; Magelhaes, P. J.; Ram, S. J. *Biophotonics Int.* **2004**, *11*, 36.
- (30) Staneva, G.; Momchilova, A.; Wolf, C.; Quinn, P. J.; Koumanov, K. *Biochim. Biophys. Acta* **2009**, *1788*, 666.
- (31) Yanagisawa, M.; Imai, M.; Masui, T.; Komura, S.; Ohta, T. *Biophys. J.* **2007**, *92*, 115.
- (32) Cahn, J. W. *Acta Metall.* **1961**, *9*, 795.
- (33) Bray, A. J. *Adv. Phys.* **2002**, *51*, 481.
- (34) Veatch, S. L.; Keller, S. L. *Biophys. J.* **2003**, *85*, 3074.
- (35) Onuki, A. *Phase Transition Dynamics*; Cambridge University Press: Cambridge, UK, 2002.
- (36) Siggia, E. D. *Phys. Rev. A* **1979**, *20*, 595.
- (37) Tanaka, H. *J. Chem. Phys.* **1996**, *105*, 10099.
- (38) Brunini, V. E.; Schuh, C. A.; Craig Carter, W. *Phys. Rev. E* **2011**, *83*, 021119.
- (39) Camley, B. A.; Brown, F. L. *Phys. Rev. Lett.* **2010**, *105*, 148102.
- (40) Tanaka, H. *Phys. Rev. Lett.* **1994**, *72*, 3690.
- (41) Tanaka, H.; Araki, T. *Phys. Rev. Lett.* **1998**, *81*, 389.
- (42) Honerkamp-Smith, A. R.; Veatch, S. L.; Keller, S. L. *Biochim. Biophys. Acta* **2009**, *1788*, 53.
- (43) Taniguchi, T. *Phys. Rev. Lett.* **1996**, *76*, 4444.
- (44) McWhirter, J. L.; Ayton, G.; Voth, G. A. *Biophys. J.* **2004**, *87*, 3242.
- (45) Laradji, M.; Sunil Kumar, P. B. *Phys. Rev. Lett.* **2004**, *93*, 198105.
- (46) Lowengrub, J. S.; Rätz, A.; Voigt, A. *Phys. Rev. E* **2009**, *79*, 031926.
- (47) Fan, J.; Han, T.; Haataja, M. *J. Chem. Phys.* **2010**, *133*, 235101.
- (48) Ngamsaad, W.; May, S.; Wagner, A. J.; Triampo, W. *Soft Matter* **2011**, *7*, 2848.
- (49) Yuan, J.; Hira, S. M.; Strouse, G. F.; Hirst, L. S. *J. Am. Chem. Soc.* **2008**, *130*, 2067.
- (50) Manley, S.; Wyss, H. M.; Miyazaki, K.; Conrad, J. C.; Trappe, V.; Kaufman, L. J.; Reichman, D. R.; Weitz, D. A. *Phys. Rev. Lett.* **2005**, *95*, 238302.
- (51) Herzig, E. M.; White, K. A.; Schofield, A. B.; Poon, W. C.; Clegg, P. S. *Nat. Mater.* **2007**, *6*, 966.
- (52) Kim, E.; Stratford, K.; Adhikari, R.; Cates, M. E. *Langmuir* **2008**, *24*, 6549.
- (53) Frolov, V. A.; Chizmadzhev, Y. A.; Cohen, F. S.; Zimmerberg, J. *Biophys. J.* **2006**, *91*, 189.
- (54) Yuan, C.; Furlong, J.; Burgos, P.; Johnston, L. J. *Biophys. J.* **2002**, *82*, 2526.
- (55) Ferraretto, A.; Pitto, M.; Palestini, P.; Masserini, M. *Biochemistry* **1997**, *36*, 9232.
- (56) Trabelsi, S.; Zhang, Z.; Zhang, S.; Lee, T. R.; Schwartz, D. K. *Langmuir* **2009**, *25*, 8056.
- (57) Schäfer, L. V.; Marrink, S. W. *Biophys. J.* **2011**, *99*, L91.